Characteristics of Torque and Suspension Force in a d-q Axis Current Control Bearingless Motor

Masahide Ooshima[a], Yuto Gomi[a]

[a] Science University of Tokyo, Suwa, 5000-1, Toyohira, Chino, Nagano, JAPAN, moshima@rs.suwa.tus.ac.jp

***Abstract*—This paper presents the characteristic of torque and suspension force in a d-q axis current control bearingless motor. It is derived based on Finite Element (FE) analysis using a simulation software, and furthermore compared with the computed results of the conventional bearingless motors, which two kinds of windings for motor drive and magnetic suspension are wound in a stator core. Three types of the conventional bearingless motor with n-pole motor winding and (n ± 2)-pole suspension winding are taken up and their computed results of the torque and suspension force are discussed in detail. As a result, the superiority of the proposed d-q axis current control bearingless motor is found.**

I. INTRODUCTION

Recently, the bearingless motors (BELMs) are attracting attention in variable speed drives due to some of its advantageous features as compared to the conventional motor drives [1]. In the BELM as there are no bearings, it is maintenance free and hence the longevity of the motor is increasing. The functions of motor and magnetic rotor levitation are successfully integrated so that the rotor shaft can be made shorter and at the same time it requires less number of inverters, controller and electric wires as compared to a motor with magnetic bearings. Thus, the overall size and cost of the bearingless machine is considerably reduced as compared to the machine with magnetic bearing. Furthermore, as the rotor shaft is shorter, there is no fear to decrease the critical speed of the BELM by the rotational axis bend.

The d-q axis current control BELM, which has been proposed by the authors, is one of the BELMs with the integrated winding [4]-[6]. The advantageous features of the proposed BELM are as follows. 1)The motor structure is just the same as the conventional brushless dc motors. The stator winding is short-pitched and hence, its distribution is quite simple. The induced voltage at the winding terminals is relatively low compared with that of the conventional BELMs with the distributed windings. From the difference of their inverter voltage ratings, the d-q axis current control BELM is competitive on the inverter cost nevertheless the number of inverters is much. In addition, the end coil length is also shorter and hence, it is superior as the rotor shaft length can be short, particularly in the two-unit tandem configuration of BELM. 2)The control method is similar to that of the interior permanent magnet synchronous motor (IPMSM), i.e., in the d-q axis current control BELM, the rotational torque is controlled by the q-axis current and the suspension force is controlled by the d-axis current (the field-weakening or field-strengthening controls). Thus, the control method is also quite simple and the general-use 3-phase inverter can be employed to control the torque and suspension force.

The authors have proposed the d-q axis current control BELM and introduced the motor structure, the principle of torque and suspension force generation and the control method. Furthermore, the validity of the proposed control method has been confirmed by the experimental test results using a prototype machine. However, the performance of motor drive and magnetic levitation in the proposed d-q axis current control BELM has not yet made clear.

In this paper, the characteristic of torque and suspension force is derived based on Finite Element (FE) analysis using a simulation software. It is compared with the computed results of the conventional BELMs, which two kinds of windings for motor drive and magnetic suspension are wound in a stator core. Three types of the conventional BELMs with n-pole motor winding and (n ± 2)-pole suspension winding are taken up; the first one is the combination of 2-pole motor drive and 4-pole magnetic suspension, the second one is the combination of 4-pole motor drive and 2-pole magnetic suspension and, the final one is the combination of 6-pole motor drive and 4-pole magnetic suspension. The characteristic of torque and suspension force in each type BELM is discussed in detail based on the computed results. From the comparison among their BELM types, it is found that the d-q axis current control BELM is absolutely superior regarding the characteristics of torque and suspension force.

II. STRUCTURE AND PRINCIPLE OF D-Q AXIS CURRENT CONTROL BEARINGLESS MOTOR

A. Motor Structure

Figure 1 shows the cross section of the proposed d-q axis current control BELM. As there is only one stator winding wound on one stator core, the structure of the d-q axis current control BELM is simple and also the winding arrangement looks like conventional blushless dc motor [4]-[6]. The stator core is classified into three sections as the section-α, the section-β and the section-γ. In the section-α, the three-phase three-wire windings $N_{u\alpha}$, $N_{v\alpha}$ and $N_{w\alpha}$ are wound; in the section-β, $N_{u\beta}$, $N_{v\beta}$ and $N_{w\beta}$ are wound; in the section-γ, $N_{u\gamma}$, $N_{v\gamma}$ and $N_{w\gamma}$ are wound. All these windings are short pitch and simple. Each section is independently controlled by separate general-use 3-phase inverters. Totally, three 3-phase inverters are needed to drive the proposed BELM. The number of inverters is much than that of the conventional BELMs. However, the capacity per an inverter may be decreased to 1/3 times that for the motor drive in the conventional BELM, and

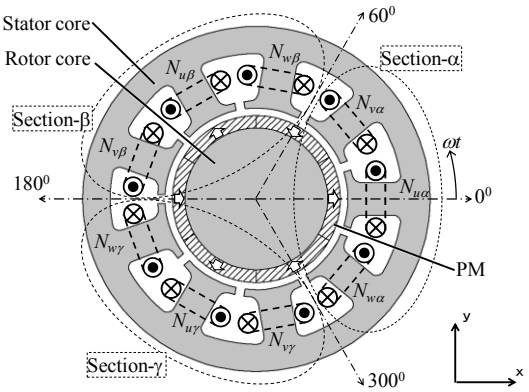

Figure 1. Cross section of a d-q axis current control bearingless motor.

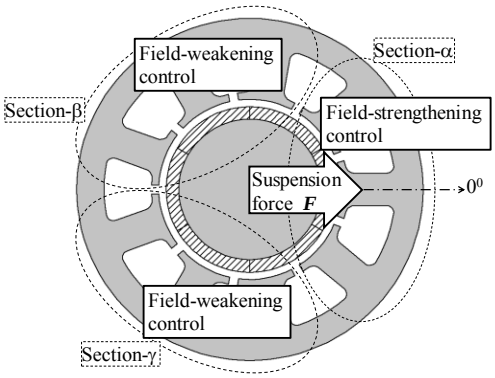

Figure 2. Principle of suspension force generation

particularly the voltage rating of inverter is lower. Thus, the d-q axis current control BELM is competitive on the inverter cost.

B. Principle of Suspension Force Generation

The suspension force is regulated to suspend the rotor of BELM. Figure 2 shows the principle of the suspension force generation in the proposed d-q axis current control BELM. The suspension force is generated by unbalanced flux density in air-gap with controlled d-axis currents $i_{d\alpha}$, $i_{d\beta}$ and $i_{d\gamma}$ in each section. For example, in section-α the field-strengthening control is done and then the air-gap flux density is increased; in the section-β and section-γ the field-weakening control is done and then the air-gap flux density is decreased. By the net vector sum in three sections, thus the suspension force is generated in the x-positive direction. By these controlled d-axis currents, the suspension force can be successfully generated in the arbitrary radial direction.

C. Control System Configuration

Figure 3 shows the control system configuration of the d-q axis current control BELM. In the motor controller, the rotor speed control method is the same as the field oriented control of the conventional ac motors. The difference $\Delta\omega$ between the detected rotor speed ω and command speed ω^* is input to the proportional-integral (PI) controller, and q-axis current command i_q^* is output of the PI speed controller which is the input to the current controllers.

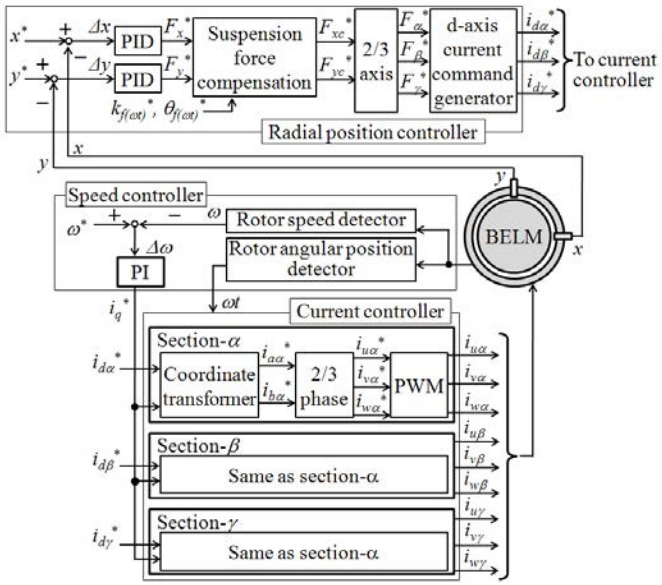

Figure 3. Control system of d-q axis current control BELM.

In the radial position controller, the detected rotor positions x and y on the x- and y- axes with eddy-current type gap sensors are input. The differences Δx and Δy between the detected rotor positions x, y and the commands x^*, y^* are input to the proportional-integral-derivative (PID) controller, and the suspension force commands F_x^* and F_y^* in the x- and y-axes coordinate are determined. In the block of suspension force compensation, F_x^* and F_y^* are significantly compensated. Because the magnitude and direction of suspension force are undesirably varied depending on the rotor angular position due to the rotation of d-axis direction. Hence, the authors have proposed the compensation method of the suspension force to stably support the rotor shaft [4]-[6]. The proposed compensation method can be explained using Figure 4. Figure 4 shows the relation between the actual suspension force $\boldsymbol{F}_{(\omega t)}$ and command force $\boldsymbol{F}_{(\omega t)}^*$. Figure 4 (a) shows the suspension forces without the compensation method. The magnitude and direction of $\boldsymbol{F}_{(\omega t)}$ does not agree with those of $\boldsymbol{F}_{(\omega t)}^*$. The ratio of the magnitude of $\boldsymbol{F}_{(\omega t)}$ to that of $\boldsymbol{F}_{(\omega t)}^*$ is defined as $k_{f(\omega t)}$, i.e., $k_{f(\omega t)}$ is shown as

$$k_{f(\omega t)} = \frac{F_{(\omega t)}}{F_{(\omega t)}^*} \tag{1}$$

Furthermore, the lead angle of $\boldsymbol{F}_{(\omega t)}$ as the reference of $\boldsymbol{F}_{(\omega t)}^*$ is defined as $\theta_{f(\omega t)}$. The $k_{f(\omega t)}$ and $\theta_{f(\omega t)}$ are defined as magnitude compensation coefficient and direction compensation coefficient, respectively.

The rotation matrix $\boldsymbol{R}_{(\omega t)}$ is defined using the $\theta_{f(\omega t)}$ as

$$\boldsymbol{R}_{(\omega t)} = \begin{bmatrix} \cos\theta_{f(\omega t)} & -\sin\theta_{f(\omega t)} \\ \sin\theta_{f(\omega t)} & \cos\theta_{f(\omega t)} \end{bmatrix} \tag{2}$$

Thus $\boldsymbol{F}_{(\omega t)}$ is represented using $k_{f(\omega t)}$, $\boldsymbol{R}_{(\omega t)}$ and $\boldsymbol{F}_{(\omega t)}^*$ as

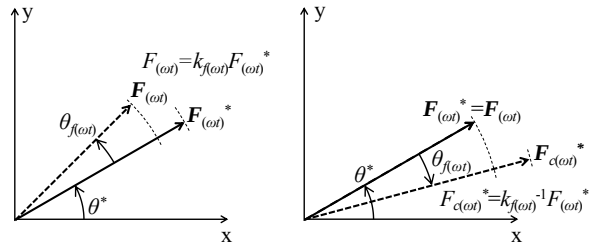

(a) Without compensation. (b) With compensation.

Figure 4. The relation between suspension force and its command.

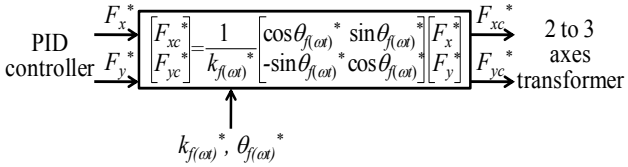

Figure 5. Block diagram of suspension force compensation.

$$\boldsymbol{F}_{(\omega t)} = k_{f(\omega t)}\boldsymbol{R}_{(\omega t)}\boldsymbol{F}_{(\omega t)}^{*} \tag{3}$$

Figure 4 (b) shows the compensated suspension force command $\boldsymbol{F}_{c(\omega t)}^{*}$. It is derived by solving for $\boldsymbol{F}_{(\omega t)}^{*}$ in the equation (3), i.e., the compensated suspension force $\boldsymbol{F}_{c(\omega t)}^{*}$ is defined as

$$\boldsymbol{F}_{\boldsymbol{c}(\omega t)}^{*} = \frac{1}{k_{f(\omega t)}}\boldsymbol{R}_{(\omega t)}^{-1}\boldsymbol{F}_{(\omega t)} \tag{4}$$

The x- and y- axes components of $\boldsymbol{F}_{c(\omega t)}^{*}$ are defined as F_{xc}^{*} and F_{yc}^{*}, respectively, so that F_{xc}^{*} and F_{yc}^{*} are shown as

$$\begin{bmatrix}F_{xc}^{*}\\F_{yc}^{*}\end{bmatrix} = \frac{1}{k_{f(\omega t)}}\begin{bmatrix}\cos\theta_{f(\omega t)} & \sin\theta_{f(\omega t)}\\ -\sin\theta_{f(\omega t)} & \cos\theta_{f(\omega t)}\end{bmatrix}\begin{bmatrix}F_x^{*}\\F_y^{*}\end{bmatrix} \tag{5}$$

By the above compensation method, $\boldsymbol{F}_{(\omega t)}$ is absolutely equal to $\boldsymbol{F}_{(\omega t)}^{*}$ as shown in Figure 4 (b). The compensated suspension force command is installed in the radial position controller so that the stable magnetic suspension is realized.

Figure 5 shows the block diagram of the suspension force compensation. The $k_{f(\omega t)}$ and $\theta_{f(\omega t)}$ are estimated from the computed results by FE analysis. They can be also done from the detected suspension force during the practical operation. The estimated $k_{f(\omega t)}$ and $\theta_{f(\omega t)}$ are input as the references $k_{f(\omega t)}^{*}$ and $\theta_{f(\omega t)}^{*}$ in the radial position controller, respectively.

These commands F_{xc}^{*} and F_{yc}^{*} are transformed into F_{α}^{*}, F_{β}^{*} and F_{γ}^{*} in the α-, β- and γ- axes coordinate. Then, the d-axis current commands $i_{d\alpha}^{*}$, $i_{d\beta}^{*}$ and $i_{d\gamma}^{*}$ are determined to be proportional to the suspension force commands, respectively.

In the current controller, the current is independently controlled in each section. In the section-α, for example, the current commands i_q^{*} and $i_{d\alpha}^{*}$ are transformed into 2-phase the current commands $i_{a\alpha}^{*}$ and $i_{b\alpha}^{*}$ in the stationary coordinate. Then $i_{a\alpha}^{*}$ and $i_{b\alpha}^{*}$ are transformed into $i_{u\alpha}^{*}$, $i_{v\alpha}^{*}$ and $i_{w\alpha}^{*}$. The winding currents $i_{u\alpha}$, $i_{v\alpha}$ and $i_{w\alpha}$ are regulated to follow the current commands in the Pulse Width Modulation (PWM) block. The current controllers of the sections -β and -γ are the same as that of the section-α.

The validation of the proposed control system has been verified by the simulated results using an FE software and the experimental test results using a prototype machine [4]-[6].

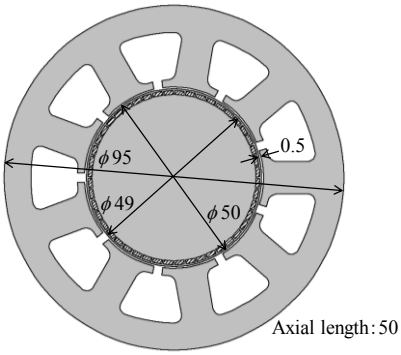

Figure 6. Dimension of FE model d-q axis current control BELM.

TABLE I. SPECIFICATION OF FE MODEL D-Q AXIS CURRENT CONTROL BELM

Rotor core, Stator core	Silicon steel
PM	Nd-Fe-B (thickness : 1 mm)
Stator winding	146 turns/tooth, ϕ0.6 mm
Current rating	1.7 A

III. CHARACTERISTICS OF TORQUE AND SUSPENSION FORCE

In this section, the torque and suspension force in a d-q axis current control BELM (d-q BELM) are computed by an FE analysis simulation software (JMAG Designer, Ver.11.1, 2-dimension) using a machine model, respectively, and the characteristic of them is obviously shown. In addition, the torque and suspension force in the conventional BELMs, which two kinds of windings for the motor drive and magnetic suspension are wound in a stator, are also computed by FE analysis. Based on the computed results, the characteristics of torque and suspension force are competitively compared and the feature of each BELM is comprehensively discussed. The combination of motor and magnetic suspension poles of the conventional BELMs is taken up to compare with the d-q axis current control BELM in this section is as follows,

- 2-pole motor and 4-pole magnetic suspension (2-4 BELM)
- 4-pole motor and 2-pole magnetic suspension (4-2 BELM)
- 6-pole motor and 4-pole magnetic suspension (6-4 BELM)

A. Specification of FE Models

Figure 6 shows the dimension of FE model of the d-q axis current control BELM. The rotor is an interior permanent magnet type (IPM), in which the small permanent magnets are buried just below the rotor core surface. The saliency ratio is relatively low and hence, the motor performance is almost the same as that of surface-mounted permanent magnet

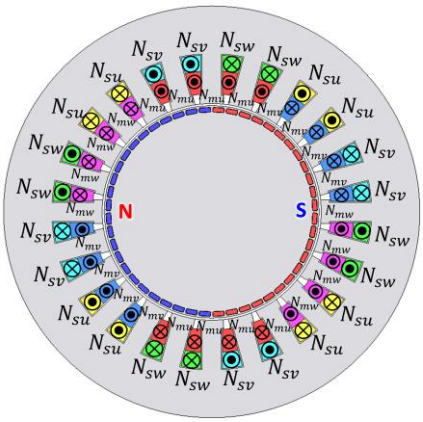

(a) 2-pole motor and 4-pole magnetic suspension (2-4 BELM).

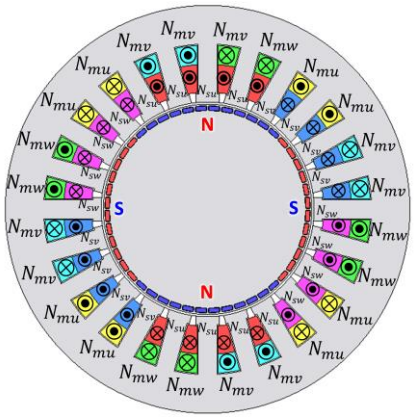

(b) 4-pole motor and 2-pole magnetic suspension (4-2 BELM).

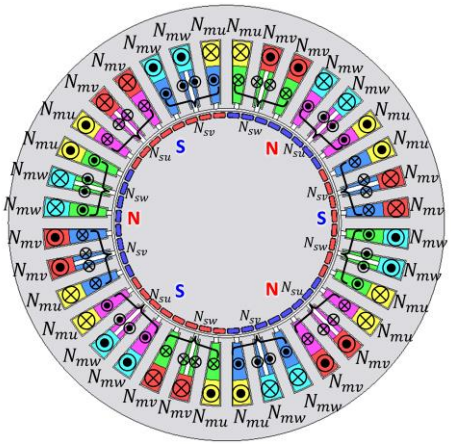

(c) 6-pole motor and 4-pole magnetic suspension (6-4 BELM).

Figure 7. Stator and rotor geometry and winding arrangement in the conventional BELMs.

synchronous motors (SPMSMs). The d-q axis current control BELM in Figure 6 is defined as a reference model to compare the characteristics of the torque and suspension force between the BELMs. Table 1 shows the specification of FE model of the d-q axis current control BELM.

Figures 7 (a)-(c) show the stator and rotor geometry and winding arrangement of the above conventional types of BELM. Figure 7 (a) shows that of the combination of 2-pole motor and 4-pole magnetic suspension. The inside windings N_{mu}, N_{mv} and N_{mw} in the stator slot are the 2-pole motor winding and the outside windings N_{su}, N_{sv} and N_{sw} are the 4-pole suspension winding. Two kinds of windings are wound in a stator core as described in Figure 7 (a). The rotor is 2-pole and its structure is basically the same as that of the reference model of d-q axis current control BELM in Figure 6.

Figure 7 (b) shows the cross section of the combination of 4-pole motor and 2-pole magnetic suspension. The outside windings N_{mu}, N_{mv} and N_{mw} are the 4-pole motor winding and the inside windings N_{su}, N_{sv} and N_{sw} are the 2-pole suspension winding. The rotor configurates 4-pole by the buried small permanent magnets.

Finally, Figure 7 (c) shows the cross section of the combination of 6-pole motor and 4-pole magnetic suspension. The outside windings N_{mu}, N_{mv} and N_{mw} are the 6-pole motor winding and the inside windings N_{su}, N_{sv} and N_{sw} are the 4-pole suspension winding. The rotor configurates 6-pole by the buried small permanent magnets.

The winding arrangement in all the above conventional BELM is a distributed winding. On the other hand, it is short-pitched in the d-q BELM. As mentioned above, there are significant differences between the d-q BELM and the conventional BELMs at the view points of the induced voltage at the winding terminals and the end coil length.

The FE models of the conventional BELMs are designed under the following conditions due to the comparison between the BELMs.

(1) In all the FE models, the outer diameter of the stator is the same as that of the model of d-q axis current control BELM. The rotor geometry is quite the same as that of the d-q BELM model except for the axial length.

(2) The maximum torque in the model of d-q axis current control BELM, i.e., the torque when the d-axis current is zero, is set as the reference torque. The conventional BELMs are designed by adjusting the axial length of the stator and rotor cores so that the maximum torque, i.e., the torque under the condition which there are no suspension windings and only motor winding occupies in the stator slots, is equal to the maximum torque of the d-q axis current control BELM. Therefore, the axial length of each FE model is different. Figure 8 shows the ratio of them.

(3) The winding current ratings are equal in all the FE models. In the d-q axis current control BELM, the ratio of the suspension force to the torque is regulated by changing the ratio of the d-axis current to the q-axis current. On the other hand, it is changed by adjusting the ratio of the number of suspension winding turns to that of the motor winding turns in the conventional BELMs. The characteristics of torque and suspension force are compared under the different conditions by changing the ratio of the torque and suspension force.

(4) The flux density in the stator yoke and teeth is less than 1.6 T. Hence, the relationship between the torque and the motor current and the relationship between the suspension force and suspension current are roughly linear under this condition, respectively.

B. Analyzed Results of Torque and Suspension Force

Figure 9 shows the relation between the computed torque

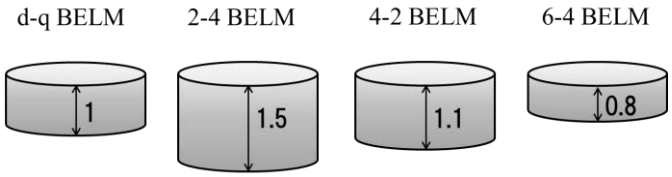

Figure 8. Ratio of axial length in FE models.

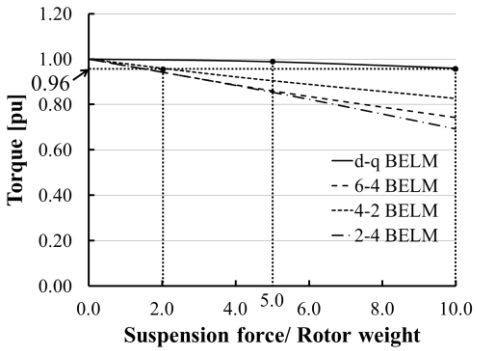

Figure 9. Characteristic of torque and suspension force .

and suspension force in the d-q axis current control BELM and the conventional BELMs. The vertical axis is the torque [p.u.] and the torque of each FE model is normalized by that when no suspension force is generated. In the d-q axis current control BELM, it is normalized by the torque when the d-axis current is set to zero, and in the other conventional BELMs, it is normalized by the torque of the FE model which there are no suspension windings in the stator core. The horizontal axis is the ratio of the suspension force to the rotor weight.

It is seen in Figure 9 that in the conventional BELMs, the torque is almost linearly decreased as the suspension force is increased by increasing the number of suspension winding turns. Because the number of motor winding turns should be decreased as the slot fill factor is remained constant. In the d-q axis current control BELM, on the other hand, the d-axis current is increased to generate the suspension force. The q-axis current should be decreased so that the winding current is within its rating. Therefore, the torque is decreased as described in Figure 9 in accordance with the increase in the suspension force. However, the decreasing ratio of the torque is less than those of the conventional BELMs. It means that the larger torque in the d-q axis current control BELM can be generated in comparison with the other BELMs when the suspension force per rotor weight is equal. In Figure 9, for example, when the suspension force per rotor weight is 5.0, the torque is decreased to less than 90% of its maximum in the conventional BELMs. However, the decreasing ratio in the d-q BELM is slightly a few percentages and the torque of d-q BELM is larger than those of the conventional BELMs.

It should be noted that the axial length of the model of 6-4 BELM is shorter than that of the d-q BELM as described in Figure 8. Hence, it is possible that its torque will be larger than that of the d-q BELM if the axial length of stator and rotor cores will be lengthened so as to be equal to that of the d-q BELM. As mentioned above, however, total axial length of the 6-4 BELM model including the end coil is significantly longer than that of d-q BELM. Because the winding arrangement of 6-4 BELM is a distributed winding. On the other hand, the winding arrangement of d-q BELM is short-pitched. Thus, it is difficult to lengthen the stator and rotor cores in the axial direction in the 6-4 BELM model.

On the contrary, the suspension force per rotor weight of the d-q BELM is larger than those of the conventional BELMs if the torque is equal. In Figure 9, for example, when the torque is 0.96 pu, the suspension force per rotor weight is 10.0 in the d-q BELM. However, it is only 2.0 even in the 4-2 BELM model, in which the suspension force per rotor weight is maximum in the conventional BELMs. The reason why the larger suspension forces than those of the other conventional BELMs is generated in the d-q BELM can be explained by the principle of d-q BELM. In the conventional BELMs, the air-gap flux densities are unbalanced by superimposing the suspension flux on the permanent magnet magnetic field. The flux density is increased in an air-gap and it is decreased in the air-gap in the opposite side across the rotor. As a result, the suspension force is successfully generated. In the d-q BELM, on the other hand, the flux densities in the air-gaps in three sections are unbalanced by the d-axis current in the sections. Hence, the suspension force in the d-q BELM is larger than those of the conventional BELMs.

From these results, the d-q axis current control BELM is absolutely superior to the conventional BELMs at the view point of the characteristics of the torque and suspension force.

IV. CONCLOSION

The characteristic of torque and suspension force in a d-q axis current control BELM has been found by the FE model calculation. Compared with those of the conventional BELMs, it is found that the proposed d-q axis current control BELM is absolutely superior. In the next step, the characteristic of torque and suspension force of the d-q axis current control BELM will be compared with several types of the conventional BELMs except for 3 conventional BELMs mentioned in this paper. Furthermore, it will be compared under the other conditions, for example, under the constant stack length of the stator and rotor cores. Based on the analyzed torque and suspension force, it will be discussed in detail which types of the BELM are more superior.

REFERENCES

[1] A. Chiba, T. Fukao, O. Ichikawa, M. Ooshima, M. Takemoto and David G. Dorrell, “Magnetic Bearings and Bearingless Drives”, Newnes Publishers, ISBN 0-7506-5727-8, March 2005.

[2] H. Grabner, S. Silber and W. Amrhein, “Feedback control of a novel bearingless torque motor using an extended FOC method for PMSMs”, 2013 IEEE International Conference on Industrial Technology (ICIT), pp.325-330, 2013.

[3] S. Silber, W. Amrhein, P. Bosch, R. Schob and N. Barletta, “Design aspects of bearingless slice motor”, IEEE/ASME Transactions on Mechatronics, Volume 10, Issue 6, pp. 611-617, 2005.

[4] Masahide Ooshima, Syunsuke Kobayashi and M. Nasir Uddin, “Magnetic Levitation Tests of a Bearingless Motor Based on d-q Axis Current Control”, *IEEE Industry Application Society 2012 Annual Meeting*, 2012-IACC-212, CDROM, @Las Vegas, 2012.

[5] Masahide Ooshima, Toshiki Karasawa and M. Nasir Uddin, “Stabilized Control Strategy Under Loaded Conditions in a d-q Axis Current Control”, *IEEE Industry Application Society 2013 Annual Meeting*, 2013-IACC-315, CDROM, @Orlando, 2013

[6] Syunsuke Kobayashi, Masahide Ooshima and M. Nasir Uddin, “A Radial Position Control Method of Bearingless Motor Based on d-q Axis Current Control”, *IEEE Transactions on Industry Applications*, vol.49, No.4, pp.1827-1835, 2013.